Bull. Astr. Soc. India (2001) **29**, 519-530

A deep VI CCD photometric study of the neglected galactic star cluster NGC 6631

Ram Sagar[1,2], B.N. Naidu[1] and V. Mohan[2]
[1] *Indian Institute of Astrophysics, Bangalore - 560 034, India*
[2] *State Observatory, Manora Peak, Nainital - 263 129, India*

Received 13 August 2001; accepted 21 November 2001

Abstract. We present the VI CCD photometric observations of about 5500 stars up to a limiting magnitude of $V \sim 20$ in an area of $\sim 16' \times 16'$ around the cluster NGC 6631. The cluster parameters determined for the first time by fitting the theoretical isochrones in the $V, (V-I)$ diagram of the cluster stars are $E(V-I) = 0.60 \pm 0.05$ mag, distance = 2.6±0.5 kpc, age = 400±100 Myr and metallicity, $Z = 0.05$. The cluster diameter determined from the radial density profile is 4.8±0.5 pc. The mass function of the cluster has a slope of 2.1±0.5.

Keywords : Photometry – Cluster NGC 6631– Colour-magnitude diagram

1. Introduction

The Galactic star clusters are valuable tools for the studies of a number of present day astrophysical problems. For such studies, a knowledge of cluster parameters and stellar content are mandatory and they are lacking for more than 60 % of the star clusters in our Galaxy. In an attempt to provide such parameters, we observed number of unstudied open star clusters from both northen and southern hemispheres. The cluster parameters derived from their deep colour magnitude digarms (CMDs) are given by Sagar & Cannon (1994), Sagar & Griffiths (1999), Subramaniam & Sagar (1999) and Sagar, Munari & de Boer (2001). In this paper, we present the first VI CCD photometric study of the NGC 6631.

The neglected open star cluster NGC 6631 ($\equiv C1824-120 \equiv$ OCL 59 $\equiv$ Lund 833) with $l = 19.^\circ47$ and $b = -0.^\circ19$ is located in the direction of Galactic center. The cluster is classified as II2m by Ruprecht (1966) and as II1m by Lyngå (1987). So far,

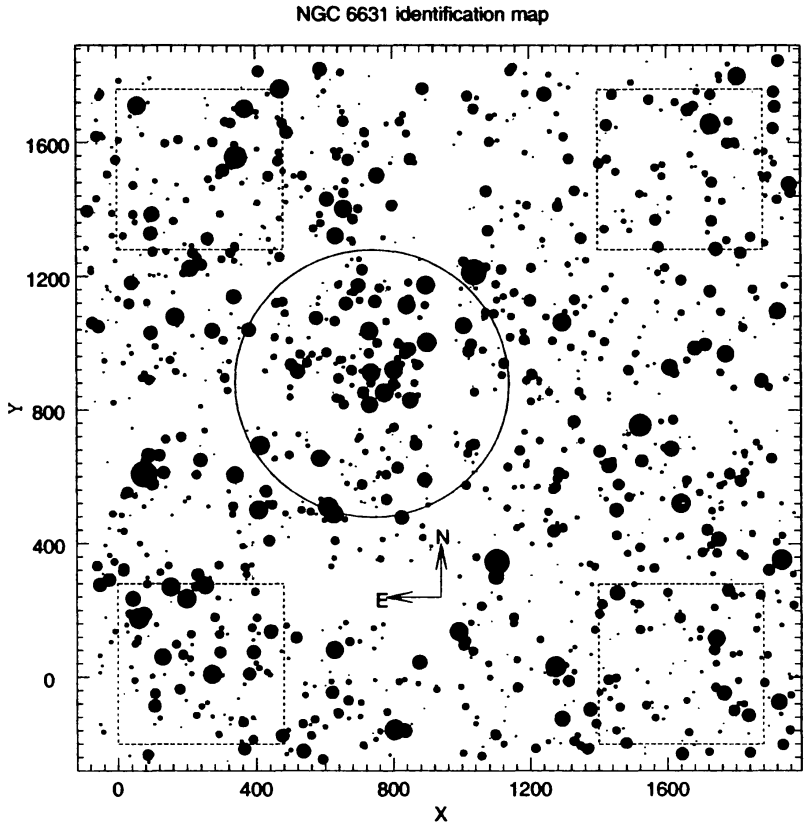

Figure 1. Identification map for the observed region around NGC 6631. The (X, Y) co-ordinates are in pixel units corresponding to $0''.48$ on the sky. North and East directions are marked. The size of star denotes the brightness, smallest size being for V = 17 mag star. Circle denotes the cluster region while dotted squares show the regions used for the study of field stars.

no photometric study has been presented for the cluster. In the Alter et al. (1970) catalogue, the angular diameter ranges from 4 to 16 arcmin while distance varies from 880 to 5000 pc, clearly indicating a large uncertainties in the parameters of NGC 6631. A deep and accurate photometric observations are therefore essential for the cluster and the same has been provided here. The details of the telescope and CCD camera used in the observations are given in the next section along with the procedures of photometric data reduction and calibration. The morphology of the CMD and parameters of the cluster are presented in the remaining part of the paper.

2. Observations and Data Reductions

The VI CCD photometric observations were obtained during May 8 to 10, 2001. For this, the mosaic CCD camera described in the accompanying paper by Naidu et al. (2001),

Table 1. Log of CCD photometric observations of the cluster NGC 6631 region and Landolt (1992) SA 107 and SA 110 standard fields.

Date	Field	Filter	Exposure in seconds
9/10 May 2001	SA 107	*I*	100×5
9/10 May 2001	SA 107	*V*	200×6
9/10 May 2001	NGC 6631	*I*	300×4
9/10 May 2001	NGC 6631	*V*	300×8
10/11 May 2001	SA 110	*I*	100×12
10/11 May 2001	SA 110	*V*	300×12

was mounted on the 104-cm Sampurnanand telescope of the State Observatory, Nainital. Each pixel of this CCD corresponds to 0.″24 at the Cassegrain focus of the f/13 telescope. The NGC 6631 was observed in Johnson V and Cousins I passbands. The area covered is about $16' \times 16'$ (see Fig. 1). For calibrating the cluster observations, two Landolt (1992) standard (SA 107 and SA 110) fields were also observed. The log of observations is given in Table 1. A number of bias and twilight flat frames were also taken to calibrate the images. The data reduction was carried out using IRAF and MIDAS softwares installed on the computers of the State Observatory, Nainital. Images were bias subtracted and flat-fielded using standard reduction techniques. As the CCD system is a mosaic of 4 CCDs, each CCD image was processed independently. The gaps of about 25″ width due to mosaic of CCDs are clearly seen in Fig. 1.

In order to improve the signal to noise ratio of the photometric measurements, the images of the cluster are aligned and co-added in each filter and also linearly rebinned with a factor of 2. The full width at half maximum of such stellar images is about 4 pixels. Although the observed cluster NGC 6631 region is not exceptionally crowded, the magnitude estimation of star has been carried out using DAOPHOT profile-fitting software, as described by Stetson (1987, 1992), so that it can be determined reliably to faint levels. The stellar PSF used by DAOPHOT is evaluated from the sum of several uncontaminated stars present in each frame. The DAOPHOT photometric errors and image parameters χ and sharpness are used to reject poor measurements. About few per cent of measured stars are rejected in this process.

The transformation equations used to transfer instrumental magnitudes to the standard photometric system are $(V - I) = p_1(v - i)_0 + q_1$ and $V = v_0 + p_2(V - I) + q_2$; where V, I are standard magnitudes taken from Landolt (1992) and v_0, i_0 are atmospheric extinction corrected instrumental CCD aperture magnitudes. p_i and q_i are the colour coefficients and zero-points respectively. For the standard fields SA 107 and SA 110 aperture photometry was performed. While observing, we placed the same set of 7 SA 110 standard stars on all the four CCDs of the mosaic. They cover a range in brightness ($11.7 < V < 14.7$) as well as in colour ($0.65 < (V - I) < 2.6$). These standard stars are used to determine p_i for the four chips of the mosaic CCD and the values are listed in Naidu et al.

Table 2. Sample of VI photometric data of the stars around the NGC 6631 cluster region. X, Y are the CCD pixel coordinates shown in Fig. 1. σ_V and σ_I are the DAOPHOT errors in the V and I bands respectively.

Star	X (pixel)	Y (pixel)	V (mag)	$(V-I)$ (mag)	σ_V (mag)	σ_I (mag)
1	−124.94	1165.81	20.41	2.81	0.37	0.05
2	−102.05	1284.94	18.63	2.43	0.08	0.01
203	−9.12	416.96	18.58	1.36	0.05	0.03
204	−8.88	−225.68	17.00	1.54	0.01	0.01
1405	393.18	1560.59	18.22	1.40	0.05	0.02
1406	393.54	1742.67	18.89	2.04	0.07	0.04

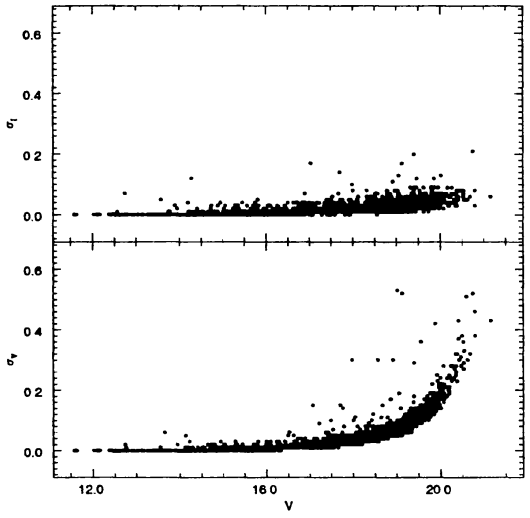

Figure 2. The DAOPHOT errors in V and I as a function of V for stars of the cluster region.

(2001). These transformation coefficients indicate that the filter combination reproduces the standard photometric system well on all the four CCDs of the mosaic camera.

Extinction coefficients and zero points were determined using the stars in the standard field of SA 107 as these were observed on the same night on which the cluster NGC 6631 was observed. The air-mass ranged from 1.2 to 2 during the observations. The magnitudes of stars in the cluster field were standardised using the slopes (p_i) obtained from the standards of SA 110 region and zero points (q_i) from those of SA 107 region.

The (X, Y) pixel coordinates, V and $(V-I)$ magnitudes of the sample stars observed in NGC 6631 are listed in Table 2 along with DAOPHOT errors. The format of the Table 2 is presented here while the entire data is available only in electronic form at the open cluster data base website at **http://obswww.unige.ch/webda/.** It can also be

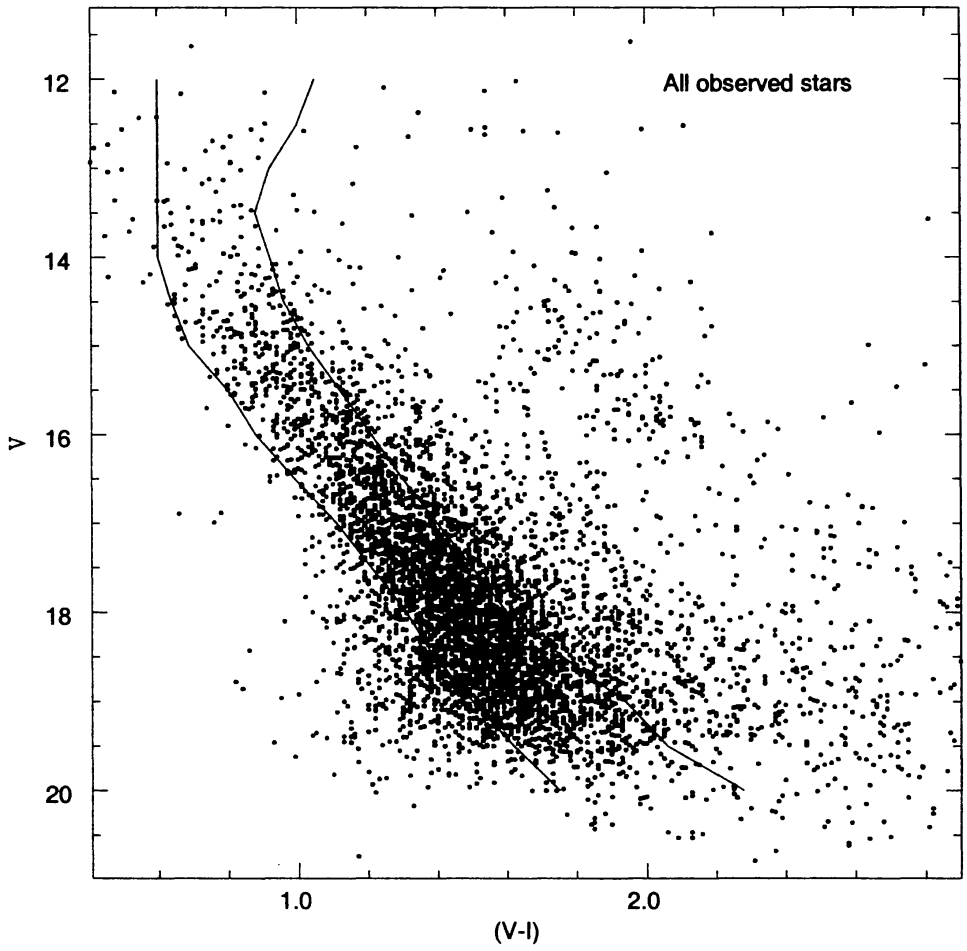

Figure 3. The $V,(V-I)$ diagram for all the measured stars around NGC 6631 with the envelopes delimiting the MS stars (see text).

obtained from the authors. Stars are numbered in the ascending order of X. There are 5533 stars observed in the region imaged by us. They are fainter than $V = 12$ mag. In Fig. 2, we plot the magnitude errors as a function of the brightness for both V and I magnitudes. The DAOPHOT errors are ~ 0.15 mag at $V = 20$ mag. We have therefore not considered stars fainter than this as the measurements are unreliable.

2.1 CMDs based on present observations

The apparent $V,(V-I)$ diagram generated from the present data is displayed in Fig. 3. The deep CMD extends down to $V = 20$ mag. A broad main-sequence (MS) and some

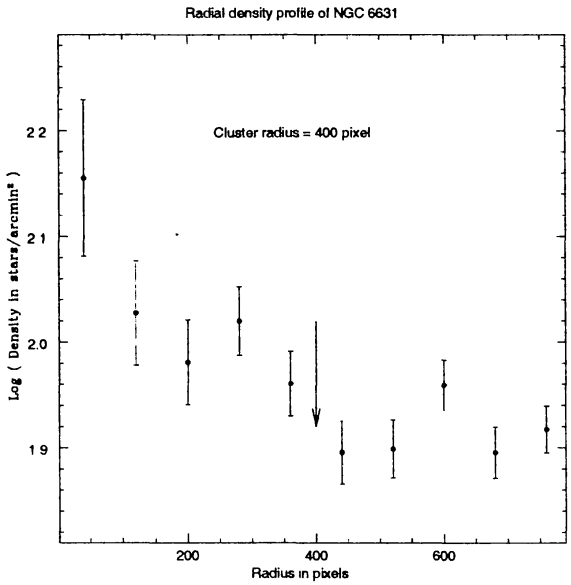

Figure 4. Plot of the stellar density profile against radius in pixels corresponding to $0''.48$ on the sky. Arrow denotes the cluster radius of 3.2 arcmin.

red gaints belonging to the both cluster and field populations are visible in the CMD. It is difficult to separate field stars from the cluster members only on the basis of their closeness to the main populated area of the CMD because field stars at cluster distance and reddening will also occupy this area. However, the possibility of cluster membership is small for the stars located well away from an eye defined blue and red envelopes of the MS (see Fig. 3). To know the actual number of cluster members from the remaining stars, their precise proper motion and/or radial velocity measurements are required. In the absence of such data, we use the statistical criteria of the cluster membership in the next section.

3. Radial stellar surface density and field star contamination

The radial variation of stellar surface density derived from the present data can be used to verify clustering, determine cluster radius and also to estimate the extent of field star contamination in the cluster region. For this, the cluster center is determined first. Its (X, Y) pixel coordinates (745,880) are derived iteratively by calculating average X and Y positions of the stars located within 200 pixels from an eye estimated center, until the values coverge. An error of few tens of pixels is expected in locating the cluster center. For determining the radial surface density of stars, the imaged area has been divided into a number of concentric circles with respect to cluster center, in such a way that each annulus region contains statistically significant number (> 40) of stars. The number density of stars in the ith annulus is given as $\rho_i = \frac{N_i}{A_i}$; where N_i is the number of stars

in the area A_i of the ith annulus. The radial density profile thus obtained is plotted in Fig. 4. The presence of clear radius density variation in the figure confirms the existence of clustering in NGC 6631.

3.1 Cluster radius

As the cluster lies in the galactic plane in the direction of Galactic center (l = 19.5°, b=−0.2°) the field star density is high with value about 85 star/arcmin^2. The peak density value in Fig. 4 is about 150 star/arcmin^2. The radius at which the value of ρ becomes approximately equal to the field star density has been considered as cluster radius and it turns out to be 3.2±0.3 arcmin. This corresponds to a linear diameter of 4.8±0.5 pc for the cluster NGC 6631. The present radius estimate agrees well with the value of 3 arcmin given by Lyngå (1987).

3.2 Field star contamination

The mosaic CCD covers a field of $\sim 16' \times 16'$. As the cluster diameter is only 6.′4, the remaining region of the field can be used to study the distribution of field stars around the cluster. For this, we use four square regions located in the four corners of the imaged field as shown in Fig. 1. Each region covers an area of 480 pixel (≡ 3.′8) square. The central pixel coordiantes of the field regions 1, 2, 3 and 4 are (240, 1520), (240, 40), (1640, 1520) and (1640, 40) respectively. The field regions thus lie at 2.1 to 3.1 cluster radius with an average value of 2.6 from the cluster center (745, 880). The frequency distribution of stars in different parts of the $V,(V-I)$ diagram of the field regions is listed in Table 3. For this, the diagram is divided into 8 magnitude bins from $V = 12$ to 20 and three colour bins with $(V-I) < 1.0, (V-I) = 1.0$ to 2.0 and $(V-I) > 2.0$. Table 3 indicates that within Poisson errors, the frequency distributions of stars in different part of the $V,(V-I)$ diagrams of all the 4 field regions agree with each other. From this, we conclude that the distribution of field stars around cluster region can be assumed uniform and the field stars contamination in the $V,(V-I)$ diagram of cluster region can be statistically estimated. The frequency distributions shown in Table 3 indicate that the present photometric observations may be considered complete only up to $V = 19$ mag.

In order to define morphological features of the cluster in the CMD accurately and also for reliable estimation of the colour excess, distance modulus and age of the cluster, we include only those stars in our further analysis which are lying within an eye defined blue and red envelopes of the MS in Fig. 3 and also within a cluster radius from the cluster center. In this way, we enhance the ratio of cluster to field stars in the sample which makes the cluster sequence better defined in the $V,(V-I)$ diagram shown in Fig. 5. To quantify the field stars still present in the diagram, the boundaries of the MS shown in Fig. 3 has been superimposed in the CMD of the both cluster and field regions. Frequency

Table 3. Frequency distributions of stars in the $V,(V-I)$ diagrams of the four field regions. The colour bins C1, C2 and C3 have $(V-I)$ values < 1.0, 1.0 to 2.0 and > 2.0 respectively.

V range (mag)	Number of stars in $(V-I)$ colour bins											
	Field 1			Field 2			Field 3			Field 4		
	C1	C2	C3	C1	C2	C3	C1	C2	C3	C1	C2	C3
12 to 13	4	0	0	2	0	2	0	2	0	2	0	0
13 to 14	6	0	0	3	0	3	2	0	0	7	0	0
14 to 15	8	5	0	6	11	2	11	17	2	14	13	0
15 to 16	23	28	0	20	25	2	11	25	4	22	18	0
16 to 17	7	65	2	9	58	8	0	61	0	11	84	0
17 to 18	4	142	13	2	114	11	0	106	7	5	132	4
18 to 19	0	202	20	2	149	25	2	171	2	0	175	4
19 to 20	2	60	19	0	57	22	2	64	21	2	65	7

Table 4. Frequency distributions of the stars in $V,(V-I)$ diagrams of the both cluster and field regions. N_{BC}, N_{MC} and N_{RC} denote the number of stars in the cluster region located blueward, near and redward of MS respectively. The corresponding numbers for the field region normalised to the cluster area are N_{BF}, N_{MF} and N_{RF} respectively. $N_C(\equiv N_{MC}-N_{MF})$ denotes statistically expected number of MS cluster members.

Range in V mag	N_{BC}	N_{BF}	N_{MC}	N_{MF}	N_{RC}	N_{RF}	N_c
12.0–13.0	1	1	7	2	4	2	5
13.0–14.0	1	1	6	4	4	1	2
14.0–15.0	4	1	20	8	8	13	12
15.0–16.0	1	0	34	23	26	22	11
16.0–17.0	8	2	52	40	30	32	12
17.0–18.0	9	12	108	75	51	49	33
18.0–19.0	30	24	127	115	43	47	12

distribution of the stars in different parts of their $V,(V-I)$ diagrams normalized for the difference in their areas is listed in Table 4. For this, the $V,(V-I)$ diagram is divided into 7 magnitude bins from $V = 12$ to 19 and three colour bins called ***blueward, near*** and ***redward*** of the MS. We find that the number of cluster MS stars is generally more than that in the field region and that the differences are mostly statistically significant, while the number of stars, which are blueward and redward of the cluster MS, in the two regions are generally similar in the statistical sense. The table indicates that the degree of field-star contamination in the MS of cluster region is increasing with faintness, as expected. Table 4 also indicates that some of the red giants brighter than $V = 13.5$ mag belong to the NGC 6631. The cluster parameters are derived using the sample stars assuming that field star contamination may not change significantly the results derived below.

4. Determination of cluster parameters

In Fig. 5, we plot the $V,(V-I)$ diagram for the sample stars. A broad but well-defined cluster MS in the magnitude range of $19 \leq V \leq 12$ and the effects of stellar evolution in the brighter stars are clearly visible. Broadening of the MS appears to be increasing with the faintness of the star. In order to see whether part of the MS broadening is due to non-uniform extinction across the cluster face or not, we divide the cluster region into four equal regions and estimate the scatter in the $V,(V-I)$ diagram of each region with respect to the isochrone adopted below for age esimate. It is found that scatter is almost similar in the CM diagrams of different cluster regions. This indicates that the inclusion of field stars, the presence of binaries, intrinsic variables and peculiar stars etc in the sample is responsible for intrinsic width of the MS though it is not possible from this study to assess their relative contributions to such a spread. As most of the factors responsible for the colour spread in the MS will redden the stars, we have used the blue envelope of the MS in CM diagram for the estimation of cluster parameters.

Bertelli et al. (1994) theoretical stellar evolutionary isochrones are used to estimate the parameters of the cluster. As the metallicity is not known spectroscopically for the cluster, we assume that it may have solar or higher metallicity, as the cluster is located in the direction of Galactic center. The isochrones fit by eye to the blue part of the long MS, turn-off point and also to a few possible red giants in Fig. 5 indicates that the metal-rich (Y=0.352, Z=0.05) ischrone of 400 Myrs (log (t) = 8.6) age fit the data reasonably well. In this process, the colour spread expected from the observational error as well as from the binarity and peculiarities has been taken into account. In order to define upper limit of the effects of binarity in Fig. 5, the isochrones which are derived from theoretical stellar evolutionary models for single stars have been brightened by 0.75 mag keeping the colour same. The isochrones fitted in this way explains the presence of stars around the MS turn-off point. This also indicates that some fraction of cluster members seems to be in the form of binaries. In stars fainter than $V = 16$ mag, strong field star contamination in the cluster MS, as also quantified in Table 4, can be clearly noticed. The values of other cluster parameters derived in this way are $E(V-I) = 0.60 \pm 0.05$ mag and $(V - M_v) = 13.5 \pm 0.3$ mag. Adopting a normal value of total to selective absorption ratio, $R(\equiv \frac{A_v}{E(V-I)}) = 2.3$, yields a true distance modulus of 12.1 ± 0.4 mag corresponding to a distance of 2.6 ± 0.5 kpc for the cluster. We expect an uncertainty of about 100 Myr in the age estimates. The errors are estimated from the errors in R, photometry, and the error in the fitting of the isochrone.

5. Mass function of the NGC 6631

The mass function (MF) of the cluster NGC 6631 is determined from the MS luminosity function of both cluster and field regions listed in Table 4. The cluster MS luminosity function corrected for field star contamination ($N_C = N_{MC} - N_{MF}$) is given in Table 4. The transformation of V to M_v and finally into mass (M) is done using cluster

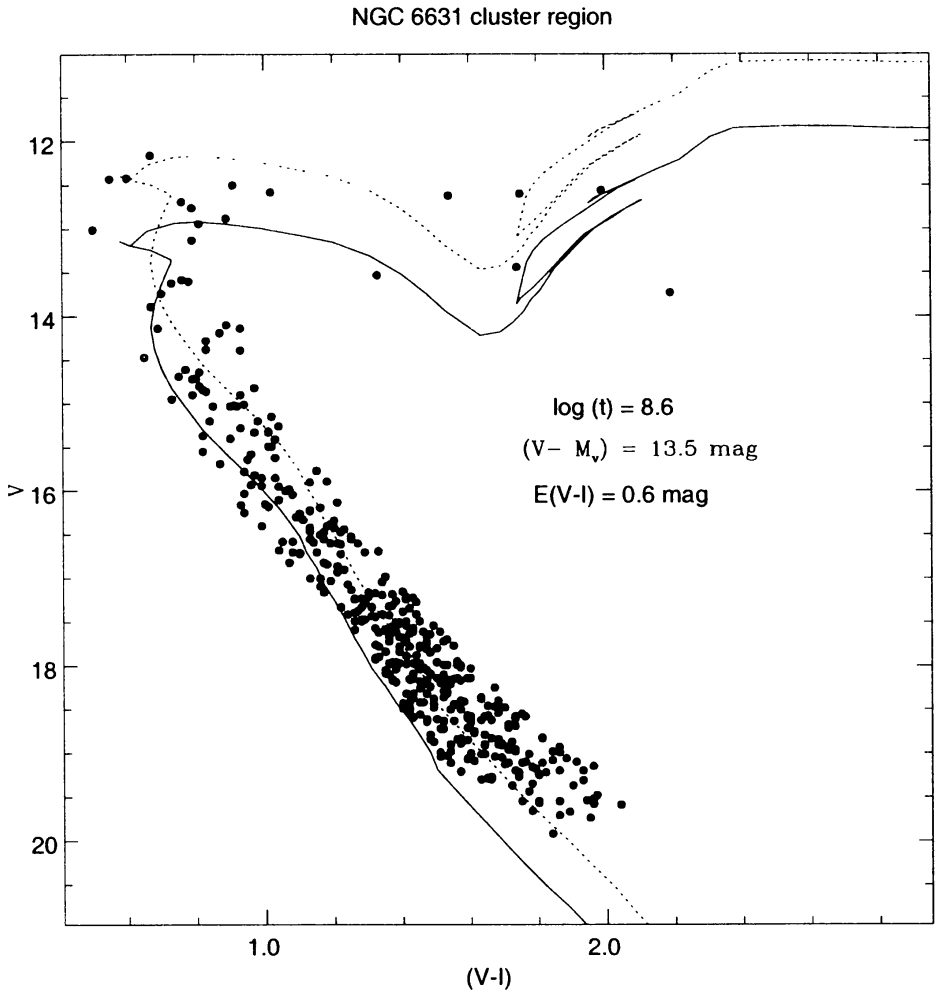

Figure 5. Theoretical isochrone given by Bertelli et al. (1994) for metallicity $Z = 0.05$ fitted to the MS, turn-off point and the red giants of NGC 6631 in $V, (V - I)$ diagram for the marked values of distance modulus, colour excess and log of age. The dotted curve shows the extent that binaries of the same mass can brighten the isochrone. All stars brighter than $V = 13.7$ mag and the MS stars of the cluster region are plotted here.

parameters derived above and the mass-luminosity relation for the isochrone of cluster age and metallicity given by Bertelli et al. (1994). The MF derived in this way is plotted in Fig. 6. The stellar MF in a limited mass interval is generally expressed as a power law $dN \propto M^{-\alpha} dM$, where dN is the number of stars in the mass interval dM and α is the slope of the MF. We therefore fit least squares linear relation to the data points which yields a value of 2.1±0.5 for the MF slope. As the Salpeter (1955) value of MF slope on this scale is 2.35, the cluster MF slope agrees with it.

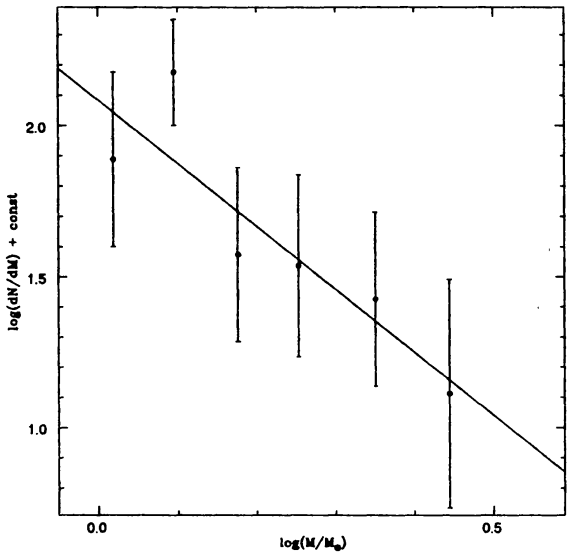

Figure 6. A plot of the NGC 6631 mass function. The bars represent $\frac{1}{\sqrt{N}}$ Poisson errors. Solid line of slope 2.1 denotes the least squares linear fit to the data points.

6. Conclusions

For the first time, the V and I CCD photometry down to $V = 20$ mag is presented for about 5,500 stars in the wide region around open cluster NGC 6631. The present work leads to the following conclusions:-

1. The visual fitting of the theoretical isochrone to the $V, (V - I)$ diagram over a broad range (~ 6) of V magnitude and also to the turn-off region yields $E(V - I) = 0.60 \pm 0.05$ mag, apparent distance modulus $= 13.5 \pm 0.3$ mag, age $= 400 \pm 100$ Myr and metallicity higher than solar.

2. The radial distribution of stellar surface density indicates that the angular radius of the cluster is 3.2 ± 0.3 arcmin and presents clear evidence for sub-clustering.

3. The slope 2.1 ± 0.5 of the cluster MF is similar to that of Salpeter (1955) MF.

4. The cluster has well defined MS. Effects of stellar evolution are clearly visible at the brighter end of the CMD. In absence of kinematical data, it is difficult to separate the cluster members from field stars unambiguously only on the basis of present observations.

5. The most probable sources for the presence of a broad main sequence in the CM diagram of the cluster are the presence of field stars, binaries, variables and peculiar stars in addition to observational errors in the sample stars.

References

Alter G., Ruprecht J., Vanysek V., 1970, Catalogue of Star Clusters and Associations, 2nd edition, Akademiai Kiado, Budapest.

Bertelli G., Bressan A., Chiosi C., Fagotto F., Nasi E., 1994, AAS, 106, 275.

Landolt A. U., 1992, AJ, 104, 340.

Lyngå G., 1987, Catalogue of open cluster data, 5th edition, 1/1 S7041, Centre de Donnees Stellaires, Strassbourg.

Naidu B.N., Srinivasan R., Mohan V., Sagar R., 2001, BASI, 29 (in press).

Ruprecht J., 1966, Bull. Astron. Inst. Czech, 17, 33.

Sagar R., Cannon R.D., 1994, BASI, 22, 381.

Sagar R., Griffiths W.K., 1999, MNRAS 299, 1.

Sagar R., Munari U., de Boer K.S., 2001, MNRAS, 327, 23.

Salpeter E.E., 1955, ApJ, 121, 161.

Stetson P.B., 1987, PASP, 99, 191.

Stetson P.B., 1992, IAU col. 136 on stellar photometry - current techniques and future developments, eds. Butler C. J & Elliott I. p 291.

Subramaniam A., Sagar R., 1999, AJ, 117, 937.